Article

pubs.acs.org/Biomac

Supported Lipid Bilayer Platform To Test Inhibitors of the Membrane Attack Complex: Insights into Biomacromolecular Assembly and Regulation

Saziye Yorulmaz,[†,‡,§] Joshua A. Jackman,[†,‡] Walter Hunziker,[§,⊥,¶] and Nam-Joon Cho*[,†,‡,∥]

[†]School of Materials Science and Engineering, Nanyang Technological University, 50 Nanyang Avenue, Singapore 639798, Singapore
[‡]Centre for Biomimetic Sensor Science, Nanyang Technological University, 50 Nanyang Drive, Singapore 637553, Singapore
[§]Institute of Molecular and Cell Biology, Agency for Science Technology and Research, Singapore 138673, Singapore
[⊥]Department of Physiology, Yong Loo Lin School of Medicine, National University of Singapore, Singapore 117599, Singapore
[¶]Singapore Eye Research Institute, Singapore 168751, Singapore
[∥]School of Chemical and Biomedical Engineering, Nanyang Technological University, 62 Nanyang Drive, Singapore 637459, Singapore

Supporting Information

ABSTRACT: Complement activation plays an important role in innate immune defense by triggering formation of the membrane attack complex (MAC), which is a biomacromolecular assembly that exhibits membrane-lytic activity against foreign invaders including various pathogens and biomaterials. Understanding the details of MAC structure and function has been the subject of extensive work involving bulk liposome and erythrocyte assays. However, it is difficult to characterize the mechanism of action of MAC inhibitor drug candidates using the conventional assays. To address this issue, we employ a biomimetic supported lipid bilayer platform to investigate how two MAC inhibitors, vitronectin and clusterin, interfere with MAC assembly in a sequential addition format, as monitored by the quartz crystal microbalance-dissipation (QCM-D) technique. Two experimental strategies based on modular assembly were selected, precincubation of inhibitor and C5b-7 complex before addition to the lipid bilayer or initial addition of inhibitor followed by the C5b-7 complex. The findings indicate that vitronectin inhibits membrane association of C5b-7 via a direct interaction with C5b-7 and via competitive membrane association onto the supported lipid bilayer. On the other hand, clusterin directly interacts with C5b-7 such that C5b-7 is still able to bind to the lipid bilayer, and clusterin affects the subsequent binding of other complement proteins involved in the MAC assembly. Taken together, the findings in this study outline a biomimetic approach based on supported lipid bilayers to explore the interactions between complement proteins and inhibitors, thereby offering insight into MAC assembly and regulation.

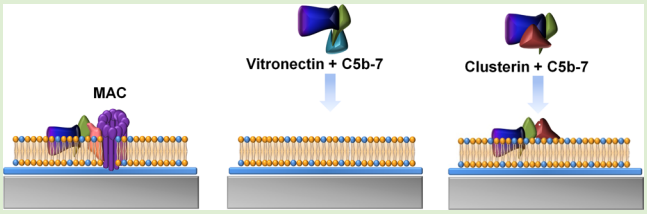

INTRODUCTION

The complement system is a key part of the innate immune system, which is involved in eliminating foreign invaders such as microbes and particulates.[1−4] Activation of the complement system, termed complement activation, consists of a proteolytic cascade involving more than 30 proteins that form macromolecular complexes in plasma and on membrane surfaces, leading to opsonization, anaphylatoxin production, and cytolysis via formation of the membrane attack complex (MAC).[2,5] Fundamentally, the mechanisms of complement activation and downstream events involve molecular recognition,[6] with surface features of various pathogens and biomaterials inducing activation through either the classical, lectin, or alternative pathway.[7,8] Recently, a number of studies[9,10] have demonstrated that *in vitro* and *in vivo* complement activation caused by biomaterials is related to surface characteristics such as the degree of hydrophobicity, surface charge density, and the presence or absence of specific functional groups.[11−16] Thus far, attention has been placed on the relationship between complement activation and biomaterial properties, with less emphasis on understanding how downstream processes such as MAC formation are affected.

The multiprotein MAC induces membrane lysis of target surfaces upon sequential association of MAC components that include C5b, C6, C7, C8, and C9 proteins.[17−19] Initially, C5b interacts with C6 and C7 in solution, leading to the formation of a stable C5b-7 complex, which can associate with target membranes via a hydrophobic domain in C7. Then, C8 and C9 proteins interact with the membrane-associated C5b-7 complex in a sequential manner to assemble the MAC, which leads to formation of a transmembrane pore that causes membrane lysis.[20−22] Because of the potent nature of the functional MAC

Received: August 5, 2015
Revised: October 3, 2015
Published: October 7, 2015

DOI: 10.1021/acs.biomac.5b01060
Biomacromolecules 2015, 16, 3594−3602

structure, human cells possess natural inhibitors in the form of soluble and membrane-bound proteins, which prevent self-destruction.[23,24] Complement inhibitors such as soluble vitronectin (S-protein), clusterin, and membrane-bound CD59 selectively block cytolytic MAC assembly.[25−29] Specifically, vitronectin and clusterin are proposed to bind to the C5b-7 precomplex, preventing its association on the cell membrane, which is a necessary step for MAC assembly.[30,31] The details of how complement inhibitors work are still being unraveled and have been the subject of significant experimental efforts.

To date, investigation of MAC assembly and its inhibition has focused on human erythrocyte and synthetic liposome studies in bulk solution. Hemolysis assays are commonly employed and provide a direct readout that is based on membrane lysis. On the other hand, to characterize formation of the MAC assembly itself, electron microscopy has been employed to examine the morphology of MAC assemblies formed by either sequential *in situ* addition of individual MAC components to lipid vesicle solutions or *in vitro* incubation of erythrocytes in human serum.[20,32] In addition, light scattering intensity measurements have followed real-time MAC assembly by tracking the interaction between MAC components in the presence or absence of lipid vesicles.[33,34] Furthermore, human, rabbit, or sheep erythrocytes have been incubated in human serum followed by detection of membrane-bound and soluble C5b-9 complexes by immunoblotting.[27,35] Collectively, the existing measurement approaches primarily support direct assessment of MAC assembly structure and functional activity. However, the existing measurement platforms are difficult to utilize to determine the mechanism of action of complement inhibitors, lending motivation to the development of new measurement platforms that address this issue, particularly in the context of blocking membrane association of MAC components.[36−38]

Toward this goal, we recently introduced a supported lipid bilayer (SLB) platform that offers label-free investigation of MAC assembly through sequential addition of purified components including the C5b-7, C8, and C9 complement proteins. Taking advantage of the compositionally flexible solvent-assisted lipid bilayer (SALB) fabrication method, the lipid composition of the SLB platform is tunable,[31,32] and it was identified that the MAC assembly preferentially forms on negatively charged lipid bilayers, in part due to the electrostatic-dependent membrane association of the C5b-7 complex.[39] A key advantage of the SLB platform is its compatibility with label-free, surface-sensitive measurement techniques such as the quartz crystal microbalance-dissipation (QCM-D) technique, which was utilized in the aforementioned study[39] and other biomacromolecular studies.[40−42] QCM-D measurements can monitor interfacial processes including complement protein adsorption and corresponding structural transformations involved in MAC assembly by tracking changes in the resonance frequency and energy dissipation of a lipid bilayer-coated, oscillating quartz crystal, which are in turn proportional to the mass and viscoelastic properties of the adsorbate, respectively.[43,44]

By expanding on the development of an SLB platform to reconstitute the MAC assembly, the goal of the present study is to investigate the quantitative stoichiometry of the MAC assembly and to determine how two known complement inhibitors, vitronectin and clusterin, function as MAC antagonists in the context of lipid membranes. Collectively, our findings support that the SLB platform in conjunction with QCM-D monitoring offers a promising approach to characterize the mechanism of action of MAC inhibitors, thereby opening the door to the classification of existing and investigational drug candidates in this class.

EXPERIMENTAL SECTION

Protein Reagents. Purified human C5b-6, C7, C8, and C9 native proteins were purchased from Complement Technology (Tyler, Texas, USA). The complement proteins were stored at −80 °C. Human recombinant clusterin (27 kDa) and vitronectin (52 kDa) proteins were obtained from Mybiosource (San Diego, California, USA) and stored at −20 °C. Recombinant vitronectin protein was received in lyophilized powder form and reconstituted at a stock concentration of 1 mg/mL in water containing 0.1 wt % bovine serum albumin (BSA). Recombinant clusterin protein was received in phosphate-buffered saline (PBS) [pH 7.4] containing 50% glycerol. Immediately before experiment, all proteins were diluted in 10 mM Tris buffer [pH 7.5] with 150 mM NaCl to the desired protein concentration.

Scheme 1. Experimental Strategies To Test Inhibitors of MAC Assembly. Two Strategies Were Employed. In the First Strategy, (i) the Inhibitor and C5b-7 Complex Were Mixed in Solution and Then (ii) the Mixture Was Added to the SLB Platform, Followed by Sequential Addition of (iii) C8 and (iv) C9 Proteins. In the Second Case, (i) the Inhibitor Was First Added to the SLB Platform Followed by Sequential Addition of (ii) C5b-7, (iii) C8, and (iv) C9 Proteins to the SLB Platform

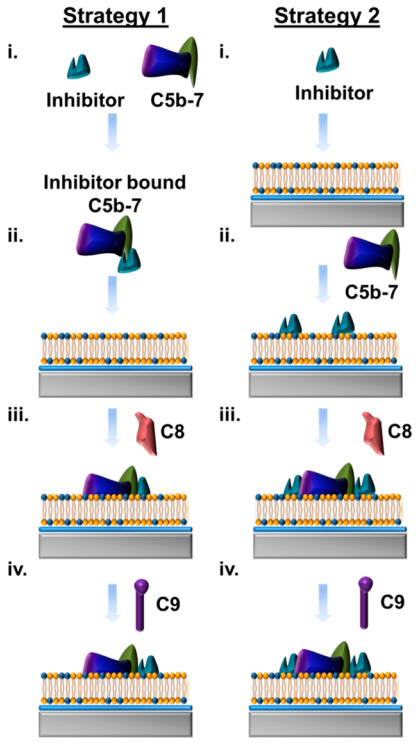

Quartz Crystal Microbalance-Dissipation. A Q-Sense E4 instrument (Q-sense AB, Gothenburg, Sweden) was utilized to monitor lipid and protein adsorption processes by tracking the changes in resonance frequency and energy dissipation of a silicon oxide-coated quartz crystal (model no. QSX303) as functions of time. The QCM-D measurement data were collected at the third, fifth, seventh, ninth, and eleventh odd overtones, and the reported QCM-D data were all obtained at the fifth overtone and normalized accordingly

DOI: 10.1021/acs.biomac.5b01060
Biomacromolecules 2015, 16, 3594−3602

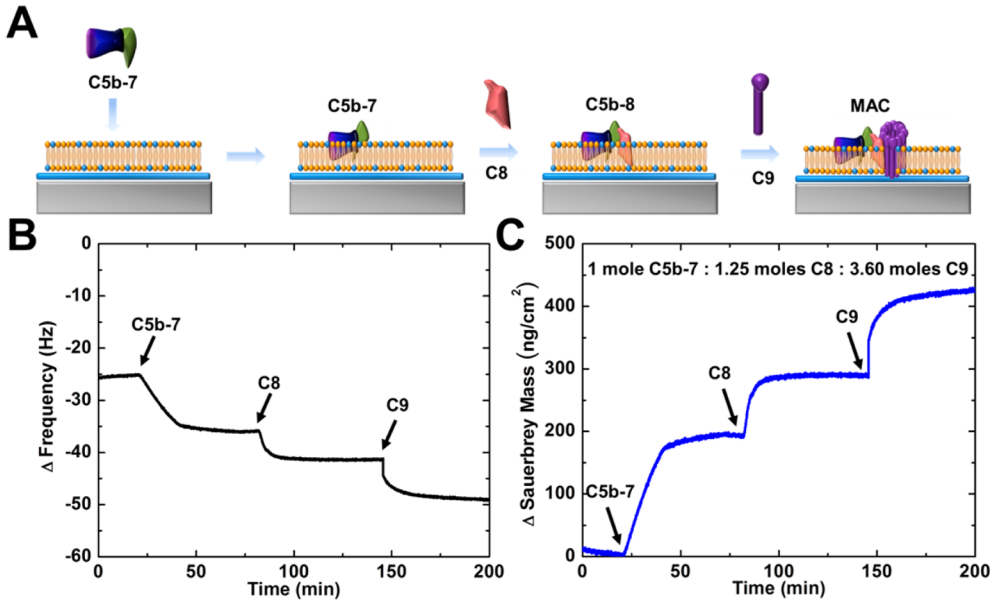

Figure 1. QCM-D monitoring of MAC assembly on the SLB platform. (A) Schematic illustration of MAC formation via sequential addition format. Changes in (B) frequency and (C) Sauerbrey mass were monitored as functions of time after sequential addition of C5b-7 complex, C8 protein, and C9 protein onto the 70:30 mol % DOPC/POPG SLB platform. The SLB on silicon oxide was initially formed by the SALB method, and then the measurement time was normalized. At t = 0 min, the MAC assay was initiated, and the C5b-7 complex was added at t = 20 min. Then, C8 protein was added at t = 80 min and C9 protein at t = 150 min. The adsorbed mass was calculated by the Sauerbrey relationship, and the mass sensitivity constant for a 1 Hz frequency shift was 17.7 ng/cm^2.

($\Delta f_{n=5}/5$). Immediately before experiment, the QCM-D sensor substrates were sequentially rinsed with 2% SDS, water, and ethanol followed by drying with nitrogen gas. The substrates were then subjected to oxygen plasma treatment (Harrick Plasma, Ithaca, NY) at the maximum radiofrequency (RF) power. All QCM-D measurements were conducted under continuous flow conditions, with the flow rate defined as 100 μL/min for all steps in the bilayer formation process and 41.8 μL/min for protein addition as controlled by a Reglo Digital peristaltic pump (Ismatec, Glattbrugg, Switzerland). The temperature of the flow cell was fixed at 24.00 ± 0.5 °C. To estimate the molecular ratio of adsorbed proteins, the Sauerbrey model was applied to convert frequency shifts into mass density values as follows:

$$\Delta m = -C\frac{\Delta f_n}{n}$$

where Δm is the adsorbate mass, C is the proportionality constant (17.7 ng/cm^2), Δf is the frequency shift, and n is the odd overtone number of the resonance frequency.[45]

Supported Lipid Bilayer Formation. The SALB formation method was used to prepare supported lipid bilayers. The 1,2-dioleoyl-*sn*-glycero-3-phosphocholine (DOPC) and 1-palmitoyl-2-oleoyl-*sn*-glycero-3-phospho-(1′-rac-glycerol) (sodium salt) (POPG) were purchased in lyophilized powder form from Avanti Polar Lipids (Alabaster, AL). Before the experiment, DOPC lipid powder was dissolved in isopropanol at a stock concentration of 10 mg/mL. POPG lipid powder was dissolved in ethanol at a stock concentration of 5 mg/mL and heated to around 40 °C to promote solubilization. Then, a 70%/30% molar fraction of DOPC and POPG lipids was prepared by mixing lipids and diluted in isopropanol to a final concentration of 0.5 mg/mL. As part of the SALB experimental protocol, a measurement baseline was first recorded in aqueous buffer solution (10 mM Tris [pH 7.5] with 150 mM NaCl (Step 1), followed by exchange with isopropanol solution (Step 2). Then, 0.5 mg/mL of lipid in isopropanol was deposited onto the substrate (Step 3), and incubated for approximately 10 min before a solvent-exchange step was performed as aqueous buffer solution was reintroduced leading to bilayer formation (Step 4). After bilayer formation, 0.1 mg/mL of BSA was added (Step 5) to verify the completeness of bilayer formation.

Membrane Attack Complex Assay. The C5b-6, C7, C8, and C9 proteins were used in a sequential addition assay format to establish the membrane attack complex on the supported lipid bilayer platform, as monitored by the QCM-D technique. Before the experiment, protein aliquots were diluted with aqueous buffer solution (10 mM Tris, 150 mM NaCl [pH 7.5]). The C5b-6 and C7 proteins were precomplexed to form a conjugate for membrane association. The C5b-7 complex was formed by mixing 20 nM C5b-6 and 50 nM C7 for a 30 min period of incubation at room temperature. Then, the C5b-7 precomplex was added to the supported lipid bilayer, followed by sequential addition of 30 nM C8 protein and then 200 nM C9 protein.

MAC Inhibitor Studies. The inhibitory effects of recombinant clusterin and vitronectin proteins on MAC assembly were evaluated by using the supported lipid bilayer platform. To investigate the mechanism of inhibition, the inhibitor proteins were individually studied and either mixed with C5b-7 precomplex or added beforehand to the supported lipid bilayer platform (Scheme 1). In the first experimental format, varying concentrations of clusterin or vitronectin between 1 and 200 nM were mixed with 20 nM C5b-7 complex and incubated at room temperature for 30 min before experiment. Then, the solution containing C5b-7 complex and inhibitor was added to the bilayer before sequential addition of C8 and C9 proteins. Alternatively, varying concentrations of clusterin or vitronectin between 1 and 200 nM were added to the bilayer followed by sequential addition of C5b-7, C8, and C9 proteins. As mentioned earlier, stock clusterin was supplied in a 50% glycerol solution. It is important to take into account the specific glycerol fraction because glycerol affects the solution viscosity, and QCM-D measurements are sensitive to changes in the viscosity of the bulk solution. For this reason, we carefully performed measurements to verify that glycerol has negligible effects on the supported lipid bilayer (Figure S1). In the clusterin experiments, the supported lipid bilayer was initially formed in pure aqueous buffer solution, and then the solution was exchanged with aqueous buffer solution, which contained a glycerol fraction equivalent to that of the clusterin solution prepared for the given experiment. Upon exchange with the glycerol–water mixture, minor frequency and dissipation shifts were observed, as expected due to the change in solution viscosity. After clusterin and C5b-7 addition was performed via either strategy, exchange with aqueous buffer solution was completed, and

DOI: 10.1021/acs.biomac.5b01060
Biomacromolecules 2015, 16, 3594–3602

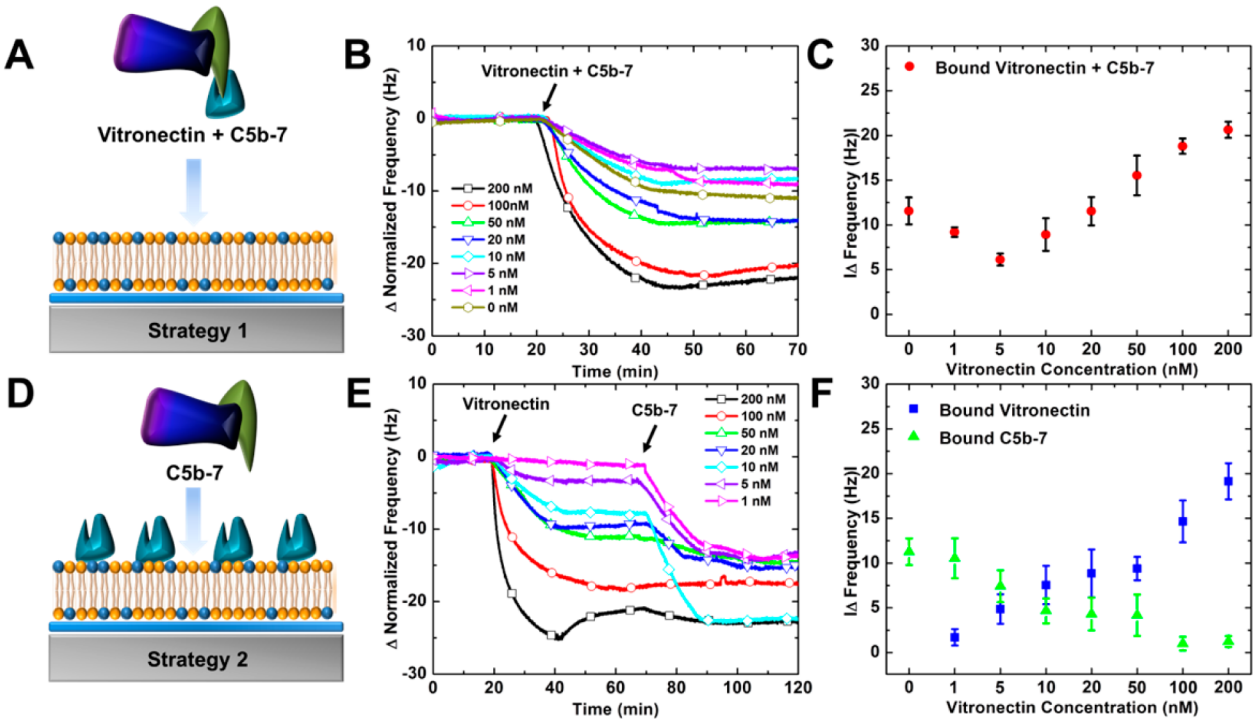

Figure 2. Influence of vitronectin on membrane association of the C5b-7 complex. (A) Schematic illustration shows addition of the C5b-7 complex, which was preincubated with vitronectin. (B) QCM-D frequency shift associated with C5b-7 + vitronectin addition to the SLB platform as a function of vitronectin concentration. The C5b-7 complex concentration was fixed at 20 nM. The proteins were added at t = 20 min. (C) Absolute value of the maximum QCM-D frequency shift due to the amount of total adsorbed protein as a function of vitronectin concentration based on the data presented in panel B. Each data point is the average + standard deviation of three independent (n = 3) measurements. (D, E) Corresponding schematic illustration and QCM-D measurement data for the addition of vitronectin to the SLB platform, followed by addition of C5b-7 complex to the same platform. (F) Absolute values of the maximum QCM-D frequency shifts due to the amounts of adsorbed vitronectin and C5b-7 complex as a function of vitronectin concentration based on the data presented in panel E. Each data point is the average + standard deviation of three independent (n = 3) measurements.

additional steps in the MAC formation process (C8 and C9 protein addition) were conducted in pure aqueous buffer solution.

RESULTS AND DISCUSSION

Design of MAC Assay Platform. To test the effect of inhibitors on MAC assembly, we first established a supported lipid bilayer platform on silicon oxide. The bilayer was fabricated by using the SALB method,[39,46,47] which involves the deposition of lipids dissolved in alcohol onto the solid support followed by solvent-exchange with aqueous buffer solution to promote bilayer formation. The selected lipid composition was 70 mol % DOPC and 30 mol % POPG to prepare negatively charged supported lipid bilayers, which support MAC assembly.[39] The QCM-D technique allows label-free measurement of the mass and viscoelastic properties of the adsorbed material, enabling detailed characterization of the fabricated lipid bilayer and each step of protein addition. After forming the lipid bilayer, the final frequency and dissipation shifts are -25.0 ± 1.4 Hz and $0.6 \pm 0.3 \times 10^{-6}$, respectively, and the values are in agreement with past reported values[39,46,47] (Figure S2). An additional step of BSA protein adsorption onto bare and bilayer-coated substrates indicated that the bilayers are >95% complete and passivated remaining parts of the substrate to specifically detect membrane association of MAC proteins to the lipid bilayer (Figure S3). Thereafter, as part of the MAC assay described in Figure 1, panel A, the change in frequency shift was recorded as a function of time upon addition of protein components of the membrane attack complex, with C5b-7, C8, and C9 proteins added in sequential format (Figure 1B).

Each stage of protein addition (indicated by the respective arrows) led to a negative frequency shift. Because the frequency shift is negatively proportional to the adsorbed mass, the frequency shifts indicate that the proteins attach to the lipid bilayer and the adsorbed mass of each protein can be quantified (Figure 1C). By taking into account the molecular weights of each protein, the molar ratio of bound proteins can be determined. On the basis of this approach, it was determined that approximately 1.25 C8 and 3.60 C9 proteins were attached to the lipid bilayer per 1 C5b-7 protein. The calculated C5b-7:C8 molar ratio is in good agreement with literature reports that indicate a 1:1 stoichiometry.[33] From these calculations, we also determined that the measured stoichiometry of the C5b-8 intermediate complex to C9 protein is 3.4, which agrees well with the literature range between 3 and 16.[27,33,48,49] Taken together, the results indicate that the platform offers a quantifiable, label-free assessment of bound protein mass, leading us to investigate how the two inhibitors each affect MAC assembly.

Effect of Vitronectin on MAC Assembly. Using the supported lipid bilayer platform, we first investigated the effect of vitronectin on membrane association of the C5b-7 complex. The C5b-7 complex and vitronectin were mixed before experiment and then added to the lipid bilayer platform (Figure 2A). With increasing vitronectin concentration, there was a general decrease in the frequency shift associated with

DOI: 10.1021/acs.biomac.5b01060
Biomacromolecules 2015, 16, 3594−3602

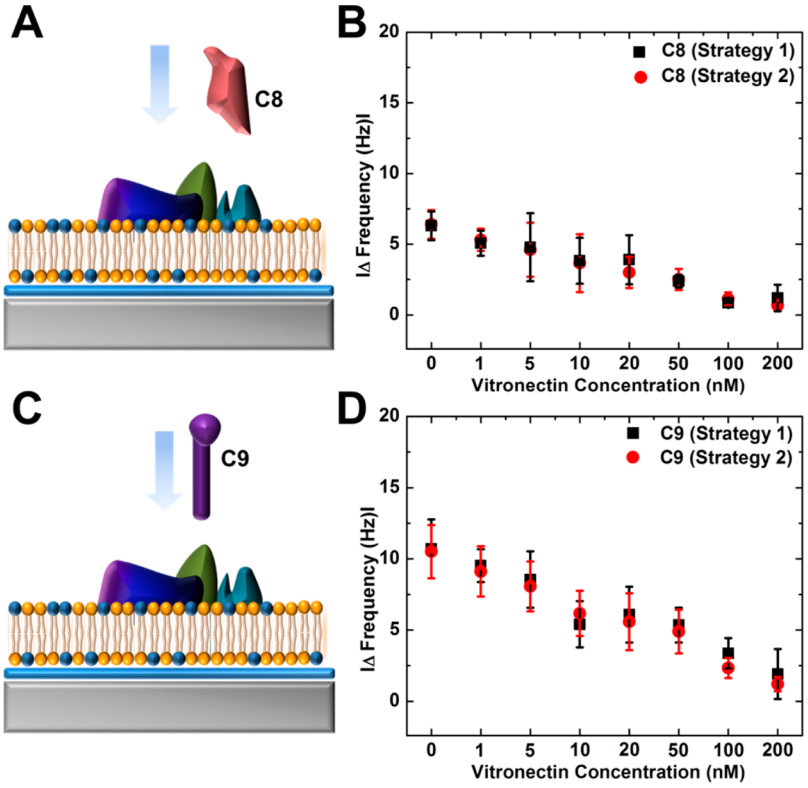

Figure 3. Effect of vitronectin on the sequential addition of C8 and C9 proteins to the SLB platform. (A) Schematic illustration of sequential addition of C8 protein to the SLB platform after vitronectin and C5b-7 addition. (B) QCM-D maximum frequency shift associated with C8 protein addition as a function of vitronectin concentration for each strategy. Each data point is the average + standard deviation of three independent (n = 3) measurements. (C, D) Corresponding schematic illustration and QCM-D measurement data for C9 protein addition as a function of vitronectin concentration.

protein adsorption (Figure 2B). To investigate details of the vitronectin concentration-dependent effects, the maximum frequency shifts are presented as a function of vitronectin concentration in Figure 2, panel C. Interestingly, at lower vitronectin concentrations (5 nM and below), the frequency shifts were lower than the value obtained from the association of C5b-7 complex in the absence of inhibitor. These results support that some of the C5b-7 complex interacted with vitronectin in the solution and lost the ability to associate on the bilayer at lower vitronectin concentration. That is, when vitronectin directly interacts with C5b-7 in solution, the resulting vitronectin-C5b-7 complex is prevented from subsequently binding to the lipid bilayer. By contrast, at higher vitronectin concentrations, there is a clear increase in the total adsorbed protein mass. In particular, at 100 nM and higher vitronectin concentrations, there are large frequency shifts, which suggest that vitronectin was the dominant adsorbed species because the C5b-7 protein concentration was fixed at 20 nM.

To clarify the effect of vitronectin on C5b-7 adsorption, a sequential addition protocol was followed in parallel experiments across the same range of inhibitor concentrations (Figure 2D). Figure 2, panel E presents the individual frequency shifts associated with membrane association of vitronectin followed by C5b-7 protein. Again, with increasing vitronectin concentration, there was an increase in vitronectin uptake. On the other hand, increasing concentrations of vitronectin inhibited subsequent membrane association of C5b-7. As presented in Figure 2, panel F, the frequency shifts were proportional to the vitronectin concentration ranging up to −19 Hz at 200 nM concentration. Likewise, prior membrane association of vitronectin suppressed membrane association of C5b-7, with negligible C5b-7 addition at high vitronectin concentrations. Particularly strong inhibition was observed at vitronectin concentrations above 50 nM. Taken together, the data obtained from both experimental strategies support that vitronectin inhibits membrane association of C5b-7 via direct interaction with C5b-7, which prevents binding to the lipid bilayer, and via competitive membrane association onto the supported lipid bilayer, which restricts the number of available adsorption sites.

Following addition of the (i) premixed C5b-7 and vitronectin or (ii) vitronectin followed by C5b-7, there was next sequential addition of C8 and C9 proteins to investigate the effect of surface-bound vitronectin. In Figure 3, the frequency shifts associated with C8 and C9 protein addition are presented as a function of vitronectin concentration. Independent of the route by which the supported lipid bilayer was treated with vitronectin, subsequent membrane association of C8 and C9 proteins decreased with increasing vitronectin concentration. There is a nearly linear trend in inhibition between 5 and 100 nM vitronectin, with minimal inhibition below this concentration range. Collectively, the results are consistent with vitronectin blocking membrane association of C5b-7, in turn preventing membrane association of C8 and C9 proteins as well.

Effect of Clusterin on MAC Assembly. In addition to vitronectin, we also studied the inhibitory effect of clusterin on membrane association of the C5b-7 complex. Initially, clusterin and C5b-7 complex were premixed and incubated for 30 min at

DOI: 10.1021/acs.biomac.5b01060
Biomacromolecules 2015, 16, 3594−3602

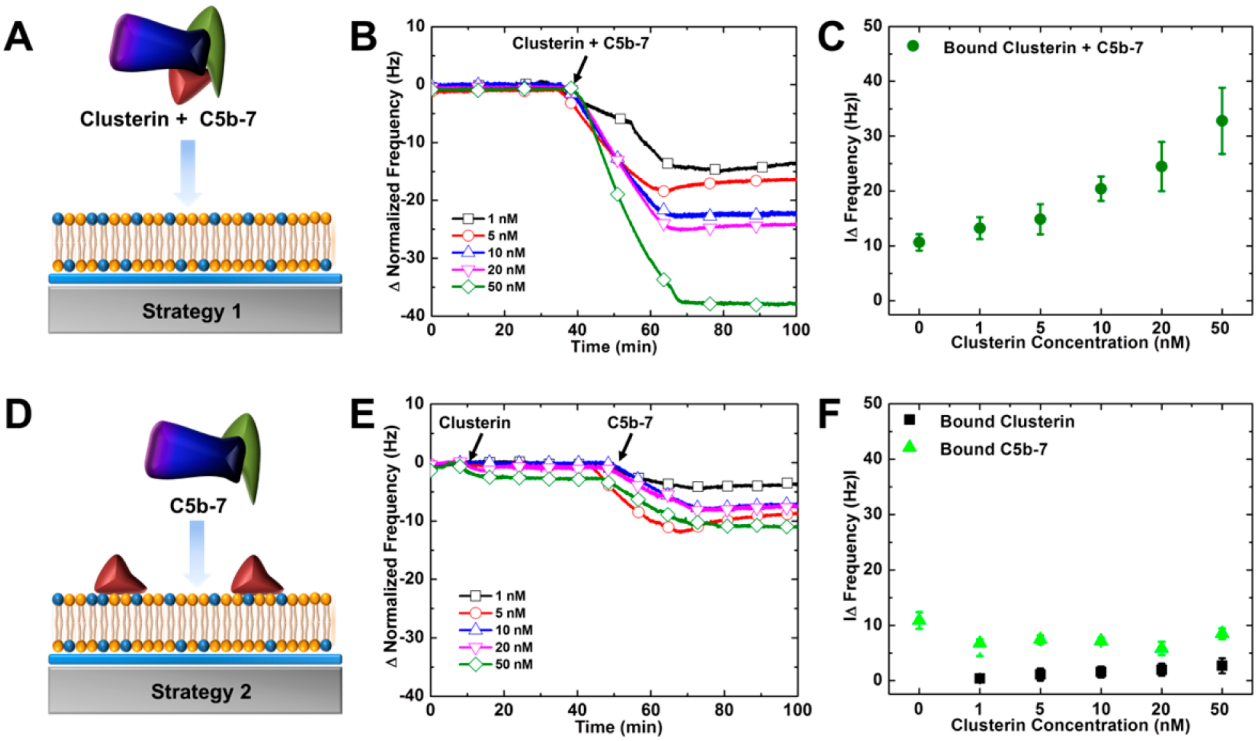

Figure 4. Influence of clusterin on membrane association of the C5b-7 complex. (A) Schematic illustration shows addition of the C5b-7 complex, which was preincubated with clusterin. (B) QCM-D frequency shift associated with C5b-7 + clusterin addition to the SLB platform as a function of vitronectin concentration. The C5b-7 complex concentration was fixed at 20 nM. The proteins were added at t = 20 min. (C) Absolute value of the maximum QCM-D frequency shift due to the amount of total adsorbed protein as a function of clusterin concentration based on the data presented in panel B. Each data point is the average + standard deviation of three independent (n = 3) measurements. (D, E) Corresponding schematic illustration and QCM-D measurement data for the addition of clusterin to the SLB platform, followed by addition of C5b-7 complex to the same platform. (F) Absolute values of the maximum QCM-D frequency shifts due to the amounts of adsorbed clusterin and C5b-7 complex as a function of clusterin concentration based on the data presented in panel E. Each data point is the average + standard deviation of three independent (n = 3) measurements.

room temperature (Figure 4A). Figure 4, panel B presents the QCM-D frequency shifts for the addition of premixed C5b-7 and clusterin to the SLB platform. With increasing clusterin concentration, there was a trend toward increased frequency shifts, as reflected in Figure 4, panel C. Low clusterin concentrations had negligible effect on protein uptake, while there was a linear correspondence between clusterin concentration and protein uptake at 10 nM clusterin and above. The data indicate that clusterin attached to the lipid bilayer together with the C5b-7 complex, clarifying a previous report,[50] which suggested that clusterin prevents attachment of C5b-7 complex to the membrane. In parallel experiments, clusterin was directly added to the supported lipid bilayer in the absence of the C5b-7 complex (Figure 4D). Even at high clusterin concentrations, there was only minimal attachment to the lipid bilayer (less than 5 Hz in all cases) (Figure 4E). In turn, the amount of attached C5b-7 on the lipid bilayer surface did not depend on the bulk clusterin concentration (Figure 4F).

To further investigate the effect of clusterin on membrane association of C8 and C9 proteins, C8 and C9 proteins were sequentially added after initial addition of premixed clusterin-C5b-7 or after sequential addition of clusterin and then the C5b-7 complex. Changes in frequency shifts associated with C8 protein addition are presented as a concentration of clusterin (Figures 5A,B). For both experimental strategies, the changes in frequency shift were largely independent of clusterin concentration at low and moderate inhibitor concentrations, whereas there was some inhibition of C8 protein attachment at high concentrations (20 nM clusterin and above). This moderate inhibitory effect of clusterin on C8 protein attachment is consistent with previous dye release experiments.[28] After C8 addition, C9 protein was next added, and the changes in frequency shifts are presented as a function of clusterin concentration (Figures 5C,D). Interestingly, the amount of bound C9 increased with increasing clusterin concentration, which is also consistent with the previous finding[25] that clusterin is known to bind to multiple sites on C9.

Comparison of Inhibition by Clusterin versus Vitronectin. Herein, we have compared the inhibitory activity of recombinant vitronectin and clusterin proteins on MAC assembly. The interaction of vitronectin and clusterin with supported lipid bilayers was determined by using the QCM-D technique. Figure 6, panel A presents the changes in attached protein mass density upon addition of vitronectin and clusterin as a function of protein concentrations. The adsorbed mass of vitronectin proteins increased when the concentration of vitronectin increased ranging from 12−344 ng/cm^2 and occurred due to electrostatic attraction because vitronectin has a positively charged domain[31] that prefers membrane association onto negatively charged lipid bilayers. However, when the C5b-7 complex was incubated with vitronectin, vitronectin blocked subsequent membrane association of the C5b-7 complex at lower concentrations, which resulted in less adsorbed protein, as reflected in Figure 6, panel B. The higher concentration of vitronectin induced an increase in total

DOI: 10.1021/acs.biomac.5b01060
Biomacromolecules 2015, 16, 3594−3602

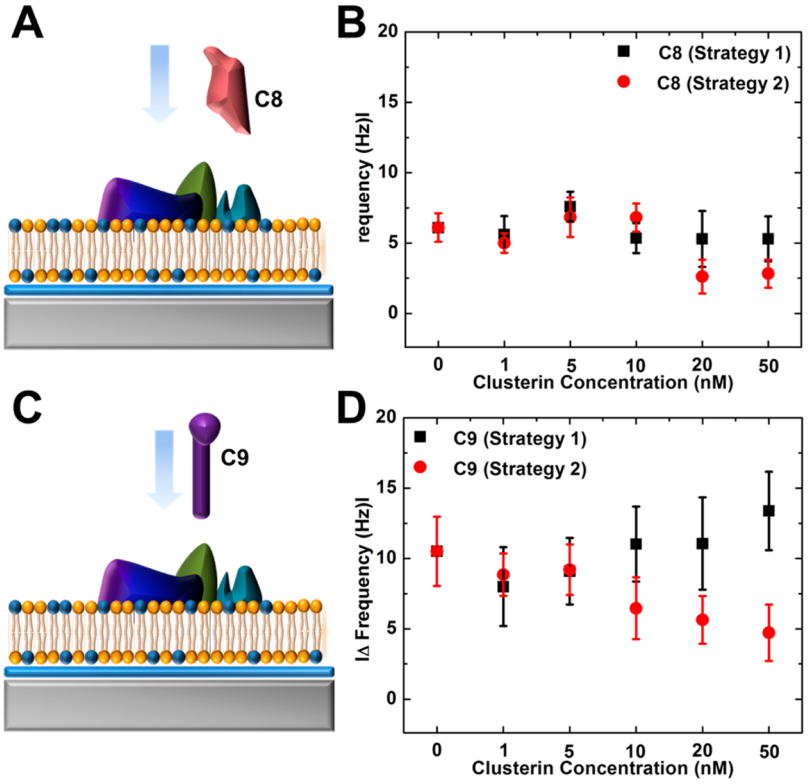

Figure 5. Effect of clusterin on the sequential addition of C8 and C9 proteins to the SLB platform. (A) Schematic illustration of sequential addition of C8 protein to the SLB platform after clusterin and C5b-7 addition. (B) QCM-D maximum frequency shift associated with C8 protein addition as a function of clusterin concentration for each strategy. Each data point is the average + standard deviation of three independent (n = 3) measurements. (C, D) Corresponding schematic illustration and QCM-D measurement data for C9 protein addition as a function of clusterin concentration.

protein attachment due to adsorption of both C5b-7 complex and vitronectin. These findings are consistent with past reports[31,51] that vitronectin inhibits MAC formation through occupation of the membrane binding site of the C5b-7 complex and extends this knowledge to directly show that vitronectin has a high propensity to attach to negatively charged lipid bilayers.

In the case of clusterin, there was only minor adsorption of the inhibitor to the SLB platform in all cases, with mass shifts always below 50 ng/cm^2 (Figure 6A). Although clusterin did not directly interact with the SLB platform, the preincubation of clusterin with the C5b-7 complex induced an appreciable change in the attached mass of total protein, which depended on the clusterin concentration, as depicted in Figure 6, panel B. On the basis of these results, we conclude that clusterin attached to the C5b-7 complex but did not block the membrane association site of the C5b-7 complex. Collectively, the QCM-D measurement results obtained on the SLB platform demonstrate that vitronectin and clusterin differentially interfere with the C5b-7 complex as part of their roles as complement inhibitors. Looking forward, there is excellent potential to utilize the SLB platform with additional sensing modalities such as combined QCM-D and electrical impedance spectroscopy measurements[52] to investigate how complement inhibitors interfere with other processes involved in MAC assembly such as pore formation.

CONCLUSION

In this study, we have investigated the association of MAC components onto the SLB platform in the presence and absence of known MAC inhibitors. First, we measured the quantitative stoichiometry of adsorbed MAC components on negatively-charged SLBs. Compared to existing attempts to determine stoichiometry from light scattering and electron microscopy, our QCM-D measurement approach yields high-precision data based on label-free mass-sensitive detection. Extending these capabilities, the specific inhibitory mechanisms of vitronectin and clusterin toward the MAC assembly were identified using a combination of two experimental strategies, which focused on the direct protein−protein interaction with the C5b-7 complex and competitive membrane association of the inhibitor to the SLB. The findings support that vitronectin blocked the membrane association of the C5b-7 complex to the SLB platform at low inhibitor concentrations through a direct interaction, whereas vitronectin at higher concentrations principally acted via competitive attachment to the SLB platform. By contrast, clusterin directly interacted with the C5b-7 complex, and the two proteins adsorbed together onto the SLB. Taken together, the results highlight the capabilities of the SLB platform to test inhibitors of the MAC assembly, generating critical mechanistic information to guide drug discovery and development with broad applicability to additional classes of inhibitors including small molecules, antibodies, and peptides.

ASSOCIATED CONTENT

Supporting Information

The Supporting Information is available free of charge on the ACS Publications website at DOI: 10.1021/acs.biomac.5b01060.

DOI: 10.1021/acs.biomac.5b01060
Biomacromolecules 2015, 16, 3594−3602

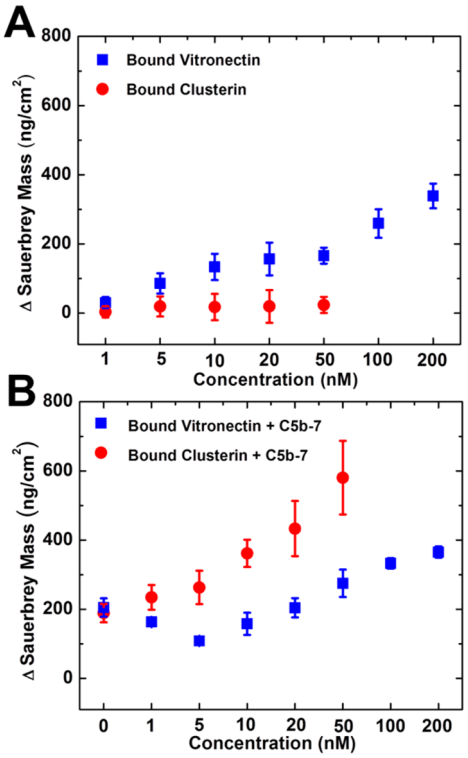

Figure 6. Comparison of inhibition by vitronectin and clusterin on membrane association of the C5b-7 complex. (A) Changes in adsorbed mass of vitronectin and clusterin upon addition to the SLB platform as a function of inhibitor concentration. (B) Changes in adsorbed mass due to inhibitor + C5b-7 complex upon joint addition to the SLB platform as a function of inhibitor concentration. Each data point is the average + standard deviation of three independent (n = 3) measurements.

QCM-D characterization of supported lipid bilayer formation and analysis of the lipid bilayer homogeneity (PDF)

AUTHOR INFORMATION

Corresponding Author

*E-mail: njcho@ntu.edu.sg.

Author Contributions

The manuscript was written through contributions of all authors. All authors have given approval to the final version of the manuscript.

Notes

The authors declare no competing financial interest.

ACKNOWLEDGMENTS

This work was supported by the National Research Foundation Grant No. NRF-NRFF2011-01, the National Medical Research Council Grant No. NMRC/CBRG/0005/2012, and the A*STAR-NHG-NTU Skin Research Grant No. SRG/14028 to N.J.C.

REFERENCES

(1) Ricklin, D.; Hajishengallis, G.; Yang, K.; Lambris, J. D. Complement: a key system for immune surveillance and homeostasis. *Nat. Immunol.* **2010**, *11*, 785−797.

(2) Rus, H.; Cudrici, C.; Niculescu, F. The role of the complement system in innate immunity. *Immunol. Res.* **2005**, *33*, 103−112.

(3) Ricklin, D.; Lambris, J. D. Therapeutic control of complement activation at the level of the central component C3. *Immunobiology* **2015**, DOI: 10.1016/j.imbio.2015.06.012.

(4) Merle, N.; Church, S. E.; Fremeaux-Bacchi, V.; Roumenina, L. T. Complement system part I−molecular mechanisms of activation and regulation. *Front. Immunol.* **2015**, *6*, 262.

(5) Morgan, B. P. The membrane attack complex as an inflammatory trigger. *Immunobiology* **2015**, DOI: 10.1016/j.imbio.2015.04.006.

(6) Gros, P. In self-defense. *Nat. Struct. Mol. Biol.* **2011**, *18*, 401−402.

(7) Ratner, B. D.; Hoffman, A. S.; Schoen, F. J.; Lemons, J. E. *Biomaterials Science: An Introduction to Materials in Medicine*; Academic press: Waltham, MA, 2004.

(8) Molino, N. M.; Bilotkach, K.; Fraser, D. A.; Ren, D.; Wang, S.-W. Complement Activation and Cell Uptake Responses Toward Polymer-Functionalized Protein Nanocapsules. *Biomacromolecules* **2012**, *13*, 974−981.

(9) Nilsson, B.; Ekdahl, K. N.; Mollnes, T. E.; Lambris, J. D. The role of complement in biomaterial-induced inflammation. *Mol. Immunol.* **2007**, *44*, 82−94.

(10) Ratner, B. D. The catastrophe revisited: blood compatibility in the 21st century. *Biomaterials* **2007**, *28*, 5144−5147.

(11) Ekdahl, K. N.; Nilsson, B.; Gölander, C. G.; Elwing, H.; Lassen, B.; Nilsson, U. R. Complement activation on radio frequency plasma modified polystyrene surfaces. *J. Colloid Interface Sci.* **1993**, *158*, 121−128.

(12) Elwing, H.; Dahlgren, C.; Harrison, R.; Lundström, I. Complement factor adsorption on solid surfaces—an ellipsometric method for investigation of quantitative aspects. *J. Immunol. Methods* **1984**, *71*, 185−191.

(13) Janatova, J.; Cheung, A.; Parker, C. Biomedical polymers differ in their capacity to activate complement. *Complement Inflamm.* **1990**, *8*, 61−69.

(14) Tengvall, P.; Askendal, A.; Ingemar, L. Complement activation by 3-mercapto-1, 2-propanediol immobilized on gold surfaces. *Biomaterials* **1996**, *17*, 1001−1007.

(15) Zhang, Y.; Wang, C.; Hu, R.; Liu, Z.; Xue, W. Polyethylenimine-Induced Alterations of Red Blood Cells and Their Recognition by the Complement System and Macrophages. *ACS Biomater. Sci. Eng.* **2015**, *1*, 139−147.

(16) Appavu, R.; Chesson, C. B.; Koyfman, A. Y.; Snook, J. D.; Kohlhapp, F. J.; Zloza, A.; Rudra, J. S. Enhancing the Magnitude of Antibody Responses through Biomaterial Stereochemistry. *ACS Biomater. Sci. Eng.* **2015**, *1*, 601−609.

(17) Bhakdi, S.; Tranum-Jensen, J. Membrane damage by complement. *Biochim. Biophys. Acta, Rev. Biomembr.* **1983**, *737*, 343−372.

(18) McGeer, P.; Akiyama, H.; Itagaki, S.; McGeer, E. Activation of the classical complement pathway in brain tissue of Alzheimer patients. *Neurosci. Lett.* **1989**, *107*, 341−346.

(19) Bhakdi, S.; Tranum-Jensen, J. Molecular nature of the complement lesion. *Proc. Natl. Acad. Sci. U. S. A.* **1978**, *75*, 5655−5659.

(20) Tschopp, J. Ultrastructure of the membrane attack complex of complement. Heterogeneity of the complex caused by different degree of C9 polymerization. *J. Biol. Chem.* **1984**, *259*, 7857−7863.

(21) Hadders, M. A.; Bubeck, D.; Roversi, P.; Hakobyan, S.; Forneris, F.; Morgan, B. P.; Pangburn, M. K.; Llorca, O.; Lea, S. M.; Gros, P. Assembly and Regulation of the Membrane Attack Complex Based on Structures of C5b6 and sC5b9. *Cell Rep.* **2012**, *1*, 200−207.

(22) Gilbert, R. J. C.; Serra, M. D.; Froelich, C. J.; Wallace, M. I.; Anderluh, G. Membrane pore formation at protein−lipid interfaces. *Trends Biochem. Sci.* **2014**, *39*, 510−516.

(23) Götze, O.; Müller-Eberhard, H. J. Lysis of erythrocytes by complement in the absence of antibody. *J. Exp. Med.* **1970**, *132* (5), 898−915.

(24) Müller-Eberhard, H. J. The killer molecule of complement. *J. Invest. Dermatol.* **1985**, *85*, 47s−52s.

(25) Tschopp, J.; Chonn, A.; Hertig, S.; French, L. Clusterin, the human apolipoprotein and complement inhibitor, binds to comple-

DOI: 10.1021/acs.biomac.5b01060
Biomacromolecules 2015, 16, 3594−3602

ment C7, C8 beta, and the b domain of C9. *J. Immunol.* **1993**, *151*, 2159−2165.
(26) Preissner, K. T.; Podack, E.; Müller-Eberhard, H. The membrane attack complex of complement: relation of C7 to the metastable membrane binding site of the intermediate complex C5b-7. *J. Immunol.* **1985**, *135*, 445−451.
(27) Bhakdi, S.; Käflein, R.; Halstensen, T.; Hugo, F.; Preissner, K.; Mollnes, T. Complement S-protein (vitronectin) is associated with cytolytic membrane-bound C5b-9 complexes. *Clin. Exp. Immunol.* **1988**, *74*, 459.
(28) McDonald, J. F.; Nelsestuen, G. L. Potent inhibition of terminal complement assembly by clusterin: characterization of its impact on C9 polymerization. *Biochemistry* **1997**, *36*, 7464−7473.
(29) Sugita, Y.; Ito, K.; Shiozuka, K.; Suzuki, H.; Gushima, H.; Tomita, M.; Masuho, Y. Recombinant soluble CD59 inhibits reactive haemolysis with complement. *Immunology* **1994**, *82*, 34−41.
(30) Tschopp, J.; Masson, D.; Schaefer, S.; Peitsch, M.; Preissner, K. T. The heparin binding domain of S-protein/vitronectin binds to complement components C7, C8, and C9 and perforin from cytolytic T-cells and inhibits their lytic activities. *Biochemistry* **1988**, *27*, 4103−4109.
(31) Milis, L.; Morris, C.; Sheehan, M.; Charlesworth, J.; Pussell, B. Vitronectin-mediated inhibition of complement: evidence for different binding sites for C5b-7 and C9. *Clin. Exp. Immunol.* **1993**, *92*, 114.
(32) Bhakdi, S.; Tranum-Jensen, J. On the cause and nature of C9-related heterogeneity of terminal complement complexes generated on target erythrocytes through the action of whole serum. *J. Immunol.* **1984**, *133*, 1453−1463.
(33) Silversmith, R. E.; Nelsestuen, G. L. The fluid-phase assembly of the membrane attack complex of complement. *Biochemistry* **1986**, *25*, 841−851.
(34) Silversmith, R. E.; Nelsestuen, G. L. Interaction of complement proteins C5b-6 and C5b-7 with phospholipid vesicles: effects of phospholipid structural features. *Biochemistry* **1986**, *25*, 7717−7725.
(35) Sheehan, M.; Morris, C.; Pussell, B.; Charlesworth, J. Complement inhibition by human vitronectin involves non-heparin binding domains. *Clin. Exp. Immunol.* **1995**, *101*, 136−141.
(36) Bubeck, D. The making of a macromolecular machine: Assembly of the membrane attack complex. *Biochemistry* **2014**, *53*, 1908−1915.
(37) Mathern, D. R.; Heeger, P. S. Molecules great and small: the complement system. *Clin. J. Am. Soc. Nephrol.* **2015**, *10*, 1636−1650.
(38) Ros, U.; García-Sáez, A. J. More than a pore: the interplay of pore-forming proteins and lipid membranes. *J. Membr. Biol.* **2015**, *248*, 545−561.
(39) Yorulmaz, S.; Tabaei, S. R.; Kim, M.; Seo, J.; Hunziker, W.; Szebeni, J.; Cho, N.-J. Membrane attack complex formation on a supported lipid bilayer: initial steps towards a CARPA predictor nanodevice. *Eur. J. Nanomed.* **2015**, *7*, 245−255.
(40) Steinmetz, N. F.; Bock, E.; Richter, R. P.; Spatz, J. P.; Lomonossoff, G. P.; Evans, D. J. Assembly of Multilayer Arrays of Viral Nanoparticles via Biospecific Recognition: A Quartz Crystal Microbalance with Dissipation Monitoring Study. *Biomacromolecules* **2008**, *9*, 456−462.
(41) Huang, C.-J.; Cho, N.-J.; Hsu, C.-J.; Tseng, P.-Y.; Frank, C. W.; Chang, Y.-C. Type I collagen-functionalized supported lipid bilayer as a cell culture platform. *Biomacromolecules* **2010**, *11*, 1231−1240.
(42) Tseng, P.-Y.; Chang, Y.-C. Tethered Fibronectin Liposomes on Supported Lipid Bilayers as a Prepackaged Controlled-Release Platform for Cell-Based Assays. *Biomacromolecules* **2012**, *13*, 2254−2262.
(43) Reviakine, I.; Rossetti, F. F.; Morozov, A. N.; Textor, M. Investigating the properties of supported vesicular layers on titanium dioxide by quartz crystal microbalance with dissipation measurements. *J. Chem. Phys.* **2005**, *122*, 204711.
(44) Cho, N.-J.; Kanazawa, K. K.; Glenn, J. S.; Frank, C. W. Employing two different quartz crystal microbalance models to study changes in viscoelastic behavior upon transformation of lipid vesicles to a bilayer on a gold surface. *Anal. Chem.* **2007**, *79*, 7027−7035.
(45) Sauerbrey, G. Verwendung von Schwingquarzen zur Wägung dünner Schichten und zur Mikrowägung. *Eur. Phys. J. A* **1959**, *155*, 206−222.
(46) Tabaei, S. R.; Jackman, J. A.; Kim, S.-O.; Zhdanov, V. P.; Cho, N.-J. Solvent-Assisted Lipid Self-Assembly at Hydrophilic Surfaces: Factors Influencing the Formation of Supported Membranes. *Langmuir* **2015**, *31*, 3125−3134.
(47) Tabaei, S. R.; Choi, J.-H.; Haw Zan, G.; Zhdanov, V. P.; Cho, N.-J. Solvent-Assisted Lipid Bilayer Formation on Silicon Dioxide and Gold. *Langmuir* **2014**, *30*, 10363−10373.
(48) Kolb, W. P.; Haxby, J. A.; Arroyave, C. M.; Müller-Eberhard, H. J. Molecular analysis of the membrane attack mechanism of complement. *J. Exp. Med.* **1972**, *135*, 549−566.
(49) Stewart, J. L.; Monahan, J. B.; Brickner, A.; Sodetz, J. M. Measurement of the ratio of the eighth and ninth components of human complement on complement-lysed membranes. *Biochemistry* **1984**, *23*, 4016−4022.
(50) Chauhan, A.; Moore, T. Presence of plasma complement regulatory proteins clusterin (Apo J) and vitronectin (S40) on circulating immune complexes (CIC). *Clin. Exp. Immunol.* **2006**, *145*, 398−406.
(51) Podack, E. R.; Müller-Eberhard, H. J. Binding of desoxycholate, phosphatidylcholine vesicles, lipoprotein and of the S-protein to complexes of terminal complement components. *J. Immunol.* **1978**, *121*, 1025−1030.
(52) Briand, E.; Zäch, M.; Svedhem, S.; Kasemo, B.; Petronis, S. Combined QCM-D and EIS study of supported lipid bilayer formation and interaction with pore-forming peptides. *Analyst* **2010**, *135*, 343−350.

DOI: 10.1021/acs.biomac.5b01060
Biomacromolecules 2015, 16, 3594−3602